Enhanced sensitivity of surface plasmon resonance biosensor for the selective detection of immunoglobin (IgG)

Awadhesh Kumar[1] · Sarvesh K. Dubey[1] · Anil Kumar[1] ·
Chandra Shekhar Pati Tripathi[1] · S. K. Srivastava[1]

Abstract

In this work, we propose a surface plasmon resonance (SPR) biosensor based on a hybrid structure of silicon nitride (Si_3N_4), molybdenum trioxide (MoO_3), and graphene oxide (GO) in the Kretschmann configuration. To investigate the performance parameters of the SPR biosensor, we calculate, theoretically, the reflectance spectra of the proposed model and analysed it. The investigation of various performance parameters i.e., sensitivity, detection accuracy, and quality factor, of sensor configuration are theoretically done with the optimized thickness of silver (55 nm), silicon nitride (5 nm), molybdenum trioxide (10 nm), and graphene oxide (2.55 nm) respectively. The sensitivity, detection accuracy, and figure of merit for the proposed SPR structure are found at 301 deg./RIU, 4.01, and 133 RIU^{-1} respectively for the detection of IgG. Furthermore, the present SPR biosensor shows improved sensitivity as compared to the other reported works. The refractive index of the analyte changes from 1.33 to 1.37 due to adsorption of the analyte at the GO surface. The proposed sensor design can detect the small change in the refractive index of the sensing media doped with the analyte.

1 Introduction

In recent days, the need for the development of biosensors is extremely important for healthcare, clinical analysis, drug discovery, environmental, security purposes, etc. (Masson 2017; Schasfoort 2017; D'Orazio 2011). It's a challenging task for biosensors to detect very low concentrations of antibodies like immunoglobulin (IgG), DNA, etc. (Kumar et al. 2022a). Recently a lot of research work have been done for the detection of IgG (Wu et al. 2016; Yang et al. 2022; Georgakilas et al. 2016). IgG is white blood cells glycoprotein molecules that are produced by plasma cells and these antibodies protect against infection. It recognizes bacteria or viruses very easily. IgG is very important for the diagnosis of

✉ S. K. Srivastava
  sanjay_itbhu@yahoo.com

[1] Department of Physics, Institute of Science, Banaras Hindu University, Varanasi 221005, India

autoimmune and immunodeficiency diseases like X-linked agammaglobulinemia and common variable immunodeficiency syndrome (Notarangelo et al. 2009; Cunningham-Rundles and Bodian 1999). In literature, various methods such as SPR, electrophoresis (Soga et al. 2003), radial immunodiffusion (Dunn et al. 2018), and immunoblotting (Mruk and Cheng 2011) have been used for the detection of IgG.

In some previously reported works, the SPR technique has been used for the detection IgG (Yang et al. 2022; Dunn et al. 2018). SPR biosensor is a good compatible sensing devices in comparison to other conventional device with high accuracy without any labeling. Surface plasmons (SPs) are charge density waves that reside at the metal-dielectric interface. The SPR is phenomenon of excitation of the free electrons at the metal-dielectric interface due to the matching of wavevector of incident light with the wavevector of surface plasma wave (SPW). In the Kretschmann configuration, generally p-polarised (TM) light is used to excite the SPs at the metal-dielectric interface. At the resonance condition, the energy of the incident light is absorbed by the SPs and results in a dip in the reflectance spectra at a particular incident angle which is called a resonance angle. The resonance angle is very responsive to the variation in concentration of the analyte in the sensing medium. Consequently, a small change in the concentration of analytes will generate a local change in the refractive index (RI) near the metallic surface and this can be explored by measuring the variation of the resonance angle (Tang et al. 2010; Englebienne et al. 2003; Homola and Piliarik 2006).

Graphene oxide (GO) has potential applications for biosensing because it has a large surface area, excellent biocompatibility (Liu et al. 2017), solubility (Wang et al. 2011), and selectivity (Loh et al. 2010). Both sp^2 and sp^3 hybrid carbon atoms are incorporated in the GO as well as it contains various oxygen-containing functional groups (Dreyer et al. 2010; Chen et al. 2012). The GO can interact in an ionic, covalent, or non-covalent way to attach with the biomolecules (Loh et al. 2010). In recent years, GO has been used to biosensors for drug delivery (Liu et al. 2009), detection of cancer cell(Liu et al. 2013), glucose (Song et al. 2013), DNA (Zhang et al. 2017), enzyme (Li et al. 2015), protein (He et al. 2013). Furthermore, to improve the SPR performances, we use a molybdenum trioxide (MoO_3) and silicon nitride (Si_3N_4) layer which can be deposited by the chemical vapor deposition (CVD) technique (Singh et al. 2021) on the desired substrate. Qiong Wu.et.al used the GO layer for attachment of the biomolecules (Wu et al. 2016) and NF Chiu et.al proposed a sensing film of the GO layer by the SPR method (Chiu et al. 2017).

MoO_3 has a wide-bandgap (~3 eV) semiconducting material and can traps electrons originating from the SPR phenomena. Furthermore, MoO_3 has unique potential applications in field sensing, photoelectronic, etc. (Peelaers et al. 2017; Morales-Luna and Morales-Luna 2020; Thomas et al. 2021). To avoid oxidation problems, we prefer to deposit silicon nitride material over the silver layer, which acts as a protective layer. Silicon nitride has a high refractive index and it has good properties such as chemical, thermal stability, and also biocompatibility (Gao et al. 1997; Luke et al. 2015).

In this paper, In the SPR biosensor, a thin metallic film of silver is coated on the base of the prism due to the easy generation of SPs on the surface (Kumar et al. 2020). Silver provides better sensitivity in comparison to gold and other plasmonic metals, owing to its high SPR ratio (ratio between the absolute values of the real and imaginary parts of the dielectric constant), but it also gets easily oxidized (Mudgal et al. 2020a). To avoid oxidation and better improvement, hybrid layers of Si_3N_4, MoO_3, and GO are deposited over the silver layer, which detects IgG effectively. A monolayer GO works as a biomolecular recognition element (BRE) for the selective attachment of IgG. The performance parameters of the proposed biosensor are investigated theoretically with the help of the transfer

matrix method. The performance parameters of the proposed structure, such as sensitivity, detection accuracy, and quality factor have been investigated. It is found that our proposed structure shows a better result in comparison with the other reported works. It has wide applications in the biomedical field for the detection of IgG and other biomolecules also.

2 Methodology

2.1 Design consideration and theoretical modeling

We have designed a "four-layer SPR biosensor'' based on the Kretschmann method, which is shown in Fig. 1. This formulated biosensor is prism coupled and based on angular inter-rogation methods. The optical wavelength is taken at 633 nm (Rahman et al. 2020). The transverse magnetic (TM) polarized light of 633 nm wavelength is incident at one face of the prism and the reflected optical signal is received by an optical detector present at another face as shown in Fig. 1. The excitation of SPs is not possible by the direct incident light, so a prism is used. Because prism provides the necessary momentum for the excita-tion of SPs at the metal-dielectric surface to the incident light for wave vector matching to generate the SPR condition (Dubey et al. 2022). BK-7 prism is easier to manufacture and has a low refractive index (Kushwaha et al. 2018a). Here prism acts as a base layer. The prism is coated with Ag having a layer thickness, $d_1 = 55$ nm by the thermal deposition technique. The Ag layer is less stable and gets oxidized easily, so an anti-reflecting material Si_3N_4 layer coated on the Ag layer with thickness, $d_2 = 5$ nm to prevent the oxidation of the silver layer. The monolayer GO enhanced the sensitivity of the proposed sensor due to it have large ability to enhance the electric field intensity and also a large surface area to cap-ture the small biomolecules (IgG) (Xiong et al. 2018). The refractive indices of different layers are considered as follows. The refractive index of the BK-7 prism can be calculated from the following relation (Brahmachari and Ray 2013)-
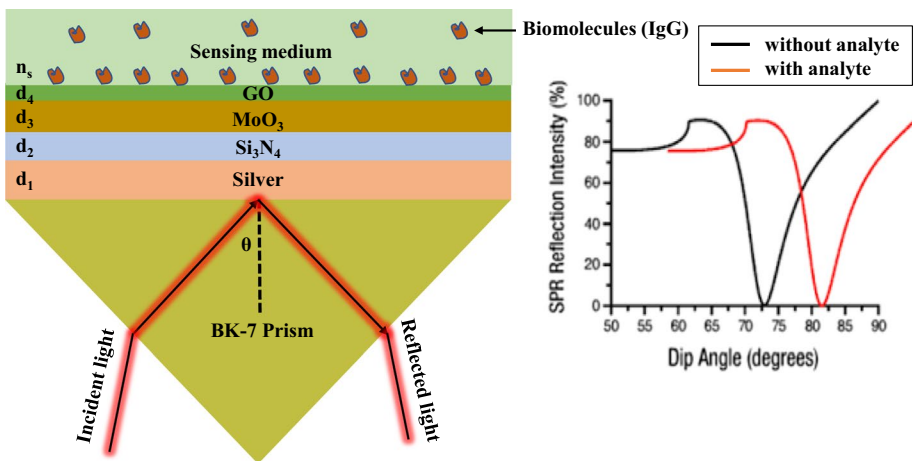

Fig. 1 Proposed configuration BK-7 prism-Ag–Si3N4–MoO₃–GO and PBS solution as sensing medium having optimize thickness

Table 1 SPR biosensor used materials, thicknesses, and RI at 633 nm

S. N	Material used	Thickness	Refractive index	References
1	Silver (Ag)	55 nm	$0.056253 + 4.2760*1i$	Balaji (2021)
2	Silicon nitride (Si_3N_4)	5 nm	2.0394	Luke et al. (2015)
3	Molybdenum trioxide (MoO_3)	10 nm	$1.8233 + 0.00204*1i$	Stelling et al. (2017)
4	Graphene oxide (GO)	2.55 nm	$1.2728 + 0.0039*1i$	Xue et al. (2013)

Table 2 SPR biosensor type of structures and layer arrangement

S. N	Structures type	Layer arrangement
1	Structure-I	Bk-7 Prism/Silver /MoO_3/GO layer
2	Structure-II	Bk-7 Prism/Silver/Silicon nitride/ MoO_3/GO layer

$$n_{BK-7} = \left(\frac{\alpha_1 \lambda^2}{\lambda^2 - \beta_1} + \frac{\alpha_2 \lambda^2}{\lambda^2 - \beta_2} + \frac{\alpha_3 \lambda^2}{\lambda^2 - \beta_3} + 1 \right)^{1/2} \tag{1}$$

where λ is the wavelength of incident light in a micrometer. This equation is only applicable for wavelengths between 0.37 to 2.5 um. The values of the constants, α_1, α_2, α_3, β_1, β_2 and β_3 are corresponding 1.0396121, 0.231792344, 1.0104694, 0.0060006986, 0.020017914, and 103.56065 respectively (Brahmachari and Ray 2013).

The refractive index of the Ag layer can be defined using the well-known Drude model for metal (Gupta and Sharma 2005).

$$n_{Ag} = \left(\varepsilon_r + i\varepsilon_i \right)^{1/2} = \left(1 - \frac{\lambda^2 \lambda_c}{\lambda_p^2 (\lambda_c + i\lambda)} \right)^{1/2} \tag{2}$$

where $\lambda_p = (1.7614 \times 10^{-5}$ m) and $\lambda_| = (1.4541 \times 10^{-5}$ m) represent the plasma and collision wavelength of the silver (Ag) layer, respectively. Furthermore, the anti-reflection coating of the Si_3N_4 layer of the optimized thickness ($Si_3N_4 = 5$ nm) (Kumar et al. 2022b) is grown over the Ag layer, which is the second layer. The refractive index value of this Si_3N_4 layer is calculated by Luke et al. (2015).

$$n_{Si_nN_4} = \left(1 + \frac{3.0249\lambda^2}{\lambda^2 - 0.1353406^2} + \frac{40314\lambda^2}{\lambda^2 - 1239.84\lambda^2} \right)^{1/2} \tag{3}$$

The next layer is taken of MoO_3 because it enhances the performance of SPR. The last layer of GO is deposited over the MoO_3 layer. The thickness and corresponding refractive index of all the layers are shown in Table 1. The Phosphate buffer solution (PBS) is considered a sensing medium. The refractive index of PBS is deliberated as $n_s = 1.343 + \Delta n_s$, where Δn_s is unstable due to the ligand-analyte interaction on the sensing surface. We have made different structures used of SPR biosensor. A comparison with the proposed work is given in Table 2.

Furthermore, we have also discussed the feasibility of the proposed SPR biosensor. For the experimental analysis, a multilayer design can be fabricated with the following procedure. A

glass prism is cleaning with the piranha solution and DI water, respectively. One face of the prism is coated with silver layer (55 nm) by a using thermal evaporation technique equipped with controlled digital thickness monitoring (Hao et al. 2020), silicon nitride and MoO_3 thin films can be deposited over desired substrate using sputtering technique (Uthanna et al. 2010). GO can be synthesized using different techniques like chemical vapour deposition (CVD), spray pyrolysis technique etc. (Manawi et al. 2018) on different substrates which can be transferred over the MoO_3 layer. Above the MoO_3 layer, the sensing medium PBS attaches to the GO surface which already contains an analyte (IgG) as shown in Fig. 1.

2.2 Mathematical modeling for reflectivity

In the SPR phenomena in the prism coupler method, when a p-polarized incident light is incident through the prism at the metal–dielectric interface, SPs are generated due to wave vector matching between the incident light wave vector $K_x = (K_0 \, n_p \sin \theta_{res})$ and the surface plasmon wave vector $K_{SP} = \left(\text{Realvalue} \sqrt{K_0(\varepsilon_m n_s^2 / (\varepsilon_m + n_s^2))} \right)$ where K_0 represent the wave vector of the incident light in free space, n_p and n_s also represents the RI of the prism and sensing medium, ε_m is the dielectric constant of the metallic layer. The necessary condition is represented as (Kumar et al. 2020).-

$$\frac{\omega}{c} \sqrt{\varepsilon_p \sin \theta_{res}} = \frac{\omega}{c} \sqrt{\varepsilon_m \varepsilon_s / (\in_m + \varepsilon_s)} \tag{4}$$

The above mathematical relation shows that the fixed operating wavelength value of the k_{SP} can be varied if the RI of the sensing medium changes. Hence, the resonance condition of SPR phenomena ($K_x = K_{SP}$) must change. At resonance angle θ_{res}, the phenomena of attenuation total internal reflection (ATR) occur by which the maximum part of incident light goes to excites SPs and results in a sharp dip in the reflectivity curve.

We have demonstrated the numerical analysis to explore the reflectance for multilayer structure using the transfer matrix method and Fresnel equation (Kushwaha et al. 2018b). Our proposed model consists of BK-7 prism, Ag, Si_3N_4, MoO_3, and GO being placed in parallel one after another. The thickness of each layer varies in the perpendicular direction the denoted as the z-axis. The boundary condition at the interface of the first layer and the last layer is considered as $Z = Z_1 = 0$ and $Z = Z_{n-1}$, respectively. The dielectric constant of the path layer equals the square of its refractive index. These methods adopt no approximation, allowing them to give accurate results rapidly. The transfer matrix expresses a relationship among the tangential components of the electric and magnetic fields of the first layer and the last layer, and the relation is given as(Kumar et al. 2020):

$$\begin{bmatrix} A_1 \\ B_1 \end{bmatrix} = P \begin{bmatrix} A_{L-1} \\ B_{L-1} \end{bmatrix} \tag{5}$$

where A_1 and B_1 represent the tangential components of electric and magnetic fields at the first layer interface. A_{L-1} and B_{L-1} represent the tangential components of electric and magnetic fields at the final layer interface. P represents the characteristic matrix of a multilayer structure with elements P_{ij}, defined as

$$P = \prod_{k=2}^{N-1} P_K = \begin{bmatrix} P_{11} & P_{12} \\ P_{21} & P_{22} \end{bmatrix} \tag{6}$$

Here

$$P_K = \begin{bmatrix} \cos\beta_P & \frac{-i}{q_K}\sin\beta_P \\ -iq_P\sin\beta_P & \cos\beta_P \end{bmatrix}$$

.where P represents an arbitrary number, β_P represents phase thickness and q_P represents refractive indices of the corresponding layers, which are explained by-

$$\beta_P = \frac{2\pi d_P}{\lambda}\sqrt{\left(\in_P - n_{BK-7}^2 \sin^2\theta_0\right)} \tag{7}$$

$$q_P = \sqrt{\left(\in_P - n_{BK-7}^2 \sin^2\theta_0\right)}/\in_P \tag{8}$$

where n_{BK-7} prism is the refractive index of the BK-7 prism, θ_0 is angle of incidence and λ as wavelength of incident light.

After some straightforward mathematical step, here we proposed of four-layer model, the reflection coefficient r_p for p-polarised light is given by

$$r_p = \frac{(P_{11} + P_{12}q_L)q_1 - (P_{21} + P_{22}q_L)}{(P_{11} + P_{12}q_L)q_1 + (P_{21} + P_{22}q_L)} \tag{9}$$

Finally, the reflectance intensity for the p- polarized incident wave and can be represented as-

$$R_p = \left|r_p\right|^2 = r_p * r_p, \tag{10}$$

2.3 Mathematical modeling of the performance parameters

The performance parameters of the SPR sensor are characterised by mainly three parameters: sensitivity (S), detection accuracy (DA), and quality parameter (Q). For the better performance of the SPR sensor, all of the above parameters should be as large as possible (Kumar et al. 2022a).

2.3.1 Sensitivity

The sensitivity is defined as the ratio of change resonance angle ($\Delta\theta$res) to change refractive index (Δn_s) and can be written as mathematically-

$$S = \Delta\theta res/\Delta n_s, \; \left[\text{Unit}: (\text{degree/RIU})\right] \tag{11}$$

2.3.2 Detection accuracy

Next, the parameters of the SPR sensor are detection accuracy (DA) or signal to noise ratio (SNR). It is expressed in terms of resonance angle change ($\Delta\theta$res) and FWHM, where FWHM means full width at half maxima as given by

$$DA = SPRangle(\Delta\theta res)/FWHM \tag{12}$$

where FWHM determine by given below relation;

FWHM $= (\theta max + \theta min)/2$, [unit: (degree)].

2.3.3 Quality factor

Another important parameter of the SPR sensor is quality factor (Q), or figure of merit (FOM), can be in terms of sensitivity (S) and FWHM given as follows;

$$Q = S/FWHM, \; \left[\text{Unit} : \left(RIU^{-1}\right)\right] \tag{13}$$

Its unit is usually expressed in (RIU^{-1}). The resonance condition phase of the reflected light also changes. The phase change at the resonance angle can be calculated by the following expression: -

$$\Phi = \arg(r) = \tan^{-1}\left[\frac{\text{Imag.}(r)}{\text{Real}(r)}\right] \tag{14}$$

Furthermore, Parameters electric field intensity enhancement factor (EFIEF) influences, and the evanescent field of both the media (metal and dielectric interface), which is defined as the ratio of the square electric field at the last interface to the first layer interface, can be calculated by the following expressed(Kumar et al. 2020).-

$$EFIEF = \left|\frac{E\left(\frac{L}{L-1}\right)}{E\left(\frac{1}{2}\right)}\right|^2 = \frac{\varepsilon_1}{\varepsilon_L}\left|\frac{H\left(\frac{L}{L-1}\right)}{H\left(\frac{1}{2}\right)}\right|^2 \tag{15}$$

where ε_1 and ε_L are dielectric constant respectively and t is the transmission coefficient.

2.3.4 Limit of detection (LOD)

It measures the change of biomolecule concentration or analyte in the sensing medium and it is defined as the given relation:

$$LOD = \Delta n_s/\Delta\theta_{res} \times 0.010° \tag{16}$$

The limit of detection is calculated for a very minute change in the sensing medium; here, we have a very small shift of 0.010°.

3 Results and discussion

Figure 1 shows the schematic diagram of the proposed SPR biosensor structure. At wavelength 633 nm, the refractive index of the taken materials with their thicknesses are mentioned in Table.1. The thickness of each layer is optimized to achieve the minimum reflectance. The minimum reflectance indicates that most of the incident light transfers to the SPs, and for any SPR sensor, the value of minimum reflectance should be nearly zero (Kumar et al. 2022c). Here, a helium–neon (He–Ne) laser of the wavelength $\lambda = 633$ nm is

used as a monochromatic source of the incident light because of the optical nonlinearity at low wavelength (Maurya et al. 2015).

Initially, we optimized the thickness of the Ag layer at a fixed thickness of the Si_3N_4 layer ($d_2 = 5$ nm) and found that the minimum reflectance occurs at a thickness of 55 nm. The optimized thickness of materials is used for the efficient excitation of surface plasmons (SPs). It is clear that from Fig. 2 the reflectance intensity depends on the thickness of the Ag layer and the optimized thickness is 55 nm as shown in Fig. 2.

We have analysed two separate hybrid structural configurations as structure-I (BK-7 prism-Ag-MoO_3-GO SPR biosensor) and structure-II (BK-7 prism-Ag-Si_3N_4-MoO_3-GO SPR biosensor) for the comparative analysis, which is given below Table 2. Basically, these two structures explain the roles of Si_3N_4, MoO_3 and GO for the performance enhancement. In our further optimization, we will study all structural configurations and their performances in our proposed biosensor.

For the structure-I, we have optimized thickness ($d_1 = 55$ nm) of the Ag layer coated on the base of the prism, which generated the SPs and gives a sharp reflectance. We further selected the MoO_3 layer ($d_3 = 10$ nm), and the monolayer graphene oxide (GO) layer ($d_4 = 2.55$ nm), over the Ag layer, respectively. Here, the MoO_3 layer improved the performance of the SPR biosensor and increased sensitivity. We have taken the last layer as a monolayer of GO. It's a thickness of 2.55 nm, because GO can be used for selective attachment of IgG. A monolayer of GO works as a bioreceptor layer for the detection of IgG as shown in Fig. 3. Over the GO layer we have considered the sensing medium (PBS solution) for sensing purposes. Here we have used phosphate buffer solution (PBS) as a sensing medium in which IgG is present. The refractive index of the sensing medium was 1.343 before adding the PBS solution. In this work, we have considered that due to the addition of IgG in the PBS solution, the refractive index of the PBS solution changes from 1.343 to 1.373 near the GO surface(Zheng et al. 2018). We have taken five different concentrations of 0, 0.025, 0.05, 0.1, and 0.25 mg/ml, respectively, of IgG in PBS solution (Kumar et al. 2022b). In Fig. 3. with an increase of IgG in the PBS solution, the corresponding resonance angle is shifted to the right side at 60.99, 64.79, 69.29, and 74.99 deg., with an RI increment of 0.03 of PBS solution due to adsorption of analyte (IgG). For Structure-I, the value of the minimum reflectivity is 2.988×10^{-3} and the resonance angle is 73.24 deg. in the bare PBS solution. After adding the IgG concentration solution to the sensing channel, the resonance angle shifts towards a higher value of 78.39 deg. with a minimum reflectivity of 1.6×10^{-2}. Thus, due to the addition of IgG in the PBS solution, the resonance angle changed by 5.15 deg. with the change in the refractive index from 1.343 to 1.373

Fig. 2 Resonance angle (deg.) verses reflectance for optimization of Ag and Si_3N_4
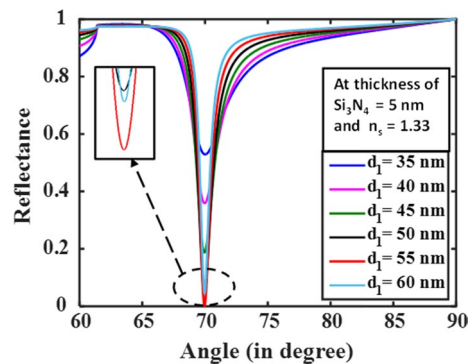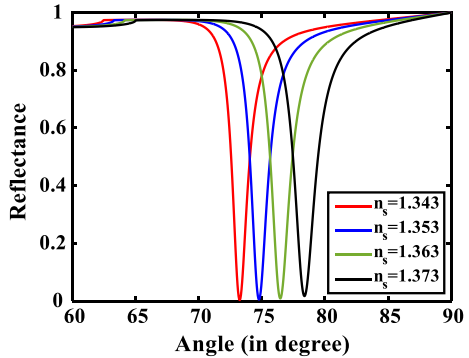
Fig. 3 Incidence angle (degree) verses reflectance for structures I

of the sensing media. If it increases the resonance angle, it means IgG attaches to the GO layer. Mathematically, sensitivity, detection accuracy, and quality factor are calculated by Eqs. (11), (12), and (13) respectively. Thus, for structure-I, the maximum sensitivity, detection accuracy, and figure of merit (FOM) are found to be 171 deg./RIU, 3.52, and 117 RIU^{-1} respectively.

Further, we used the phase interrogation method to check the resonance angle, which is described mathematically as Eqs. (14), whose results support our findings. Moreover, we have studied the phase change of the reflected light versus incident angle at different concentrations of IgG, such as 0, 0.025, 0.05, 0.1, and 0.25 mg/ml, adding in the sensing medium then increased the resonance angle, respectively for the proposed structure-I as shown in Fig. 4. It is clear from Fig. 4 an abrupt phase change is contained at the same resonance angle when the refractive index increases from (1.343 to 1.373) in the sensing medium. The position of the phase change is found to be sensitive to the concentration of the analyte (IgG). As we change the concentration of the IgG, the corresponding phase change position shift towards the higher angle side because of the damping of SPs for structure-I.

The electric field intensity enhancement factor (EFIEF) is very important performance parameter of the SPR biosensor and as well as defines how much the electric field is limited in the sensing medium in comparison to the metal-dielectric interface. The EFIEF allows the field to peak height at the resonance angle. Mathematically, EFIEF is calculated from Eq. (15). Figure 5 shows, if increasing the concentration of the IgG, i.e., (0, 0.025, 0.05, 0.1, and 0.25 mg/ml), the effective RI of the sensing medium changes from 1.343
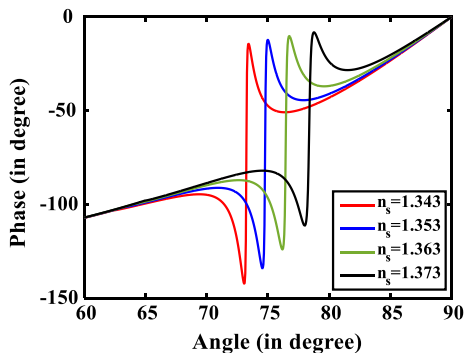

Fig. 4 Phase vs incident angle for structures I

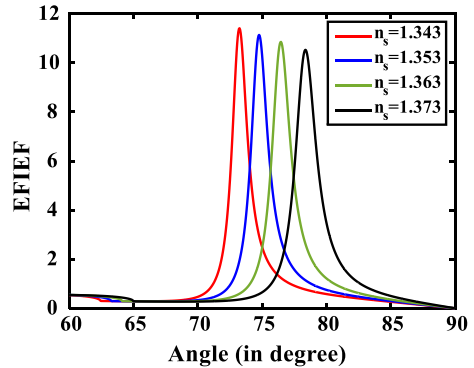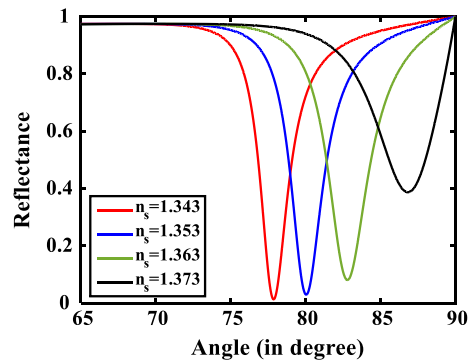**Fig. 5** Resonance angle (degree) verses EFIEF for structures-I

Fig. 6 Incidence angle (degree) verses reflectance for structure-II


to 1.373, the resulting EFIEF decreases. It is clearly seen that the excitation of SPs occurs because, at the resonance angle, most of the incident light energy is transferred to the sensing probe for the generation of the SPs. Here, we can say that IgG strongly attaches to the GO layer and increases the refractive index of the sensing medium of the biosensor. The decrease in EFIEF with the concentration of IgG occurs mainly due to the absorption of incident energy by the IgG. In this study, we have taken the fixed thickness of the GO layer and changed the concentration of IgG. Figure 5 shows the variation of EFIEF of the proposed biosensor with the refractive index of the sensing medium for the design structure-I.

In order to further improve the performance parameters of the above configurations, we have proposed structure-II of the SPR biosensor, which consists of BK-7 prism-Ag-Si_3N_4-MoO_3-GO-sensing medium. At the constant thickness of the Si_3N_4 of 5 nm, it is clearly seen that as we increased the thickness of Ag the reflectance dip gets increases and becomes sharper at 55 nm. Figure 6 depicts that the minimum reflectivity and corresponding resonance angle of 77.85 deg. for the bare PBS buffer solution are 1.337×10^{-2}. After adsorption of the IgG, the minimum reflectivity is increased to 3.871×10^{-1} and the resonance angle shifted to a higher angle of 86.88 deg. The maximum resonance angle change is 9.03 deg. due to a concentration change of 0.25 mg/ml of IgG. Therefore, we can say that IgG is attached strongly to the GO layer, because GO has a large surface area and high electron mobility with an increased electric field between analyte and contact surface. Hence, the sensitivity, detection accuracy, and quality factor are increasing in the SPR biosensor. The GO layer is selective for the

Table 3 The performance parameters of the proposed SPR biosensors

S. N	Used structure	$\Delta\theta$ (deg.)	FWHM	Sensitivity (deg./RIU)	Detection accuracy (DA)	Quality factor (QF) (RIU^{-1})
A	Structure-I	5.15	1.46	171	3.52	117
B	Structure-II	9.03	2.25	301	4.01	133

Fig. 7 Phase vs incident angle for structures-II
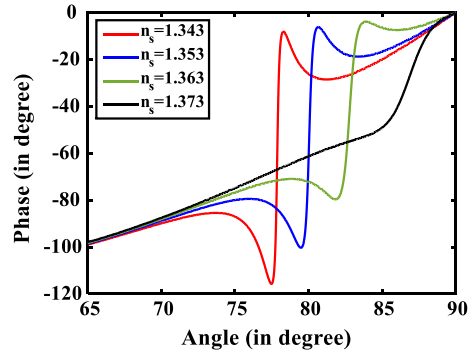
attachment for the detection of IgG due to its excellent biocompatibility. For this configuration, the maximum achieved sensitivity is 301 deg./RIU with a detection accuracy of 4.01 and a quality factor of 133 RIU^{-1}. It's clear that structure-II is better than structure-I due to the large real value of the dielectric constant of Si_3N_4, MoO_3, and monolayer GO. Thus, Si_3N_4 is responsible for the enhancement in the parameters in structure-II as compared to structure-I. The performance parameters of all the structures at wavelength of 633 nm are summarised in Table 3.

Figure 7 shows the phase change of the reflected light versus incidence angle for the proposed multilayer structure. It is clear that for the structure-II, an abrupt phase change occurs at the same resonance angle for the different concentration of the IgG as
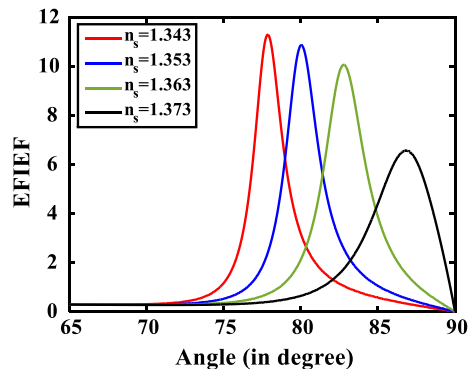
Fig. 8 Resonance angle (degree) vs EFIEF for structures-II

Table 4 A Comparative analysis of our proposed work with the parameters using different materials

S.N	BK-7 prism + material used	S (deg./RIU)	DA	QF (RIU^{-1})	LOD ($\times 10^{-5}$)	References
1	ZnO + Au + MoS$_2$ + graphene	101.5	1.81	15.11	–	Kushwaha et al. (2018a)
2	ZnO + Ag + Au + BaTiO$_3$ + graphene	116.6	4.54	37.87	–	Mudgal et al. (2020b)
3	Au + GO	143.0	0.16	23.72	–	Raikwar et al. (2020)
4	Au/BlueP + MoS$_2$ + antimonene	194.8	0.15	–	–	Singh et al. (2020)
5	Ag + Au + Franckeite + TMDC + BP	208	0.08	17.33	–	Srivastava and Prajapati (2020)
6	Ag + Si$_3$N$_4$ + GO	171	3.52	117	5.82	This work
7	Ag + Si$_3$N$_4$ + MoO$_3$ + GO	301	4.01	133	3.32	This work

in Fig. 6, which support our finding results. With the change in concentration of IgG, the corresponding phase changing position shifts to the higher angle side due to the alteration of the RI of sensing medium, and hence the resonance condition for the SPs also changes the position of resonance.

For the structure-II of EFIEF, Fig. 8 clear that with the increasing concentration of IgG in the sensing medium, the RI of n_s changes from 1.343 to 1.373, then the EFIEF decreases, which occurs due to the strong adsorption of IgG at the sensing surface of the biosensor. The decrease in EFIEF with the concentration of IgG occurs due to the absorption of incident energy by the IgG.

Thus, we have found the performance parameters of the SPR biosensor for the above structures I and II. The parameters such as sensitivity, detection accuracy, and quality factor for both the structures are tabulated in Table 3 and with a comparative study, other reported work is summarised in Table 4. We have also calculated the limit of detection (LOD) from Eq. (16) for the proposed the structures I and II, which are found to be 5.82×10^{-5} and 3.32×10^{-5} deg. respectively.

4 Conclusion

In the present work, we have proposed a multilayer Ag-Si_3N_4-MoO_3-GO based SPR biosensor for the detection of IgG. In this work, monolayer GO is used for the selective attachment of IgG. It is found that the proposed biosensor shows improved sensitivity, quality parameter, and detection accuracy as compared to the other reported SPR biosensors for the dynamic change of refractive index (n_s) from 1.343 to 1.373. Furthermore, Si_3N_4 and MoO_3 are used for performance enhancement due to their unique properties. As the real part of the dielectric constant of these materials is larger compared to their imaginary parts, there is minimal loss of surface plasmons. The proposed structure shows maximum sensitivity, quality parameter, and detection accuracy as 301 deg./RIU, 133 RIU^{-1}, and 4.01 respectively. Also, a proposed SPR biosensor can be fabricated for real-time and level-free detection of IgG, which would be inexpensive.

Data availability Not applicable.

Code availability Not applicable.

Declarations

Conflict of interest The authors declare no competing interests.

Ethical approval It is an original study. No living subjects were involved in this work. Currently, this manuscript is not submitted for review to any other journal. this draft will not submit elsewhere before a decision is made by this journal.

Consent of participate No human subjects were involved in this study.

References

Balaji, V.: Theoretical analysis of tuning and sensitivity improvement of surface plasmon resonance biosensor employing heterostructures of titanium disilicide and graphene. J. Comput. Electron. **21**, 263–269 (2021)

Brahmachari, K., Ray, M.: Effect of prism material on design of surface plasmon resonance sensor by admittance loci method. Front. Optoelectron. **6**, 185–193 (2013)

Chen, D., Feng, H., Li, J.: Graphene oxide: preparation, functionalization, and electrochemical applications. Chem. Rev. **112**, 6027–6053 (2012)

Chiu, N.-F., Fan, S.-Y., Yang, C.-D., Huang, T.-Y.: Carboxyl-functionalized graphene oxide composites as SPR biosensors with enhanced sensitivity for immunoaffinity detection. Biosens. Bioelectron. **89**, 370–376 (2017)

Cunningham-Rundles, C., Bodian, C.: Common variable immunodeficiency: clinical and immunological features of 248 patients. Clin. Immunol. **92**, 34–48 (1999)

D'Orazio, P.: Biosensors in clinical chemistry: 2011 update. Clin. Chim. Acta **412**, 1749–1761 (2011)

Dreyer, D.R., Park, S., Bielawski, C.W., Ruoff, R.S.: The chemistry of graphene oxide. Chem. Soc. Rev. **39**, 228–240 (2010)

Dubey, S.K., Kumar, A., Kumar, A., Pathak, A., Srivastava, S.: A study of highly sensitive D-shaped optical fiber surface plasmon resonance based refractive index sensor using grating structures of Ag-TiO2 and Ag-SnO2. Optik **252**, 168527 (2022)

Dunn, A., Duffy, C., Gordon, A., Morrison, S., Argüello, A., Welsh, M., Earley, B.: Comparison of single radial immunodiffusion and ELISA for the quantification of immunoglobulin G in bovine colostrum, milk and calf sera. J. Appl. Anim. Res. **46**, 758–765 (2018)

Englebienne, P., Van Hoonacker, A., Verhas, M.: Surface plasmon resonance: principles, methods and applications in biomedical sciences. Spectroscopy **17**, 255–273 (2003)

Gao, H., Luginbühl, R., Sigrist, H.: Bioengineering of silicon nitride. Sens. Actuators B Chem. **38**, 38–41 (1997)

Georgakilas, V., Tiwari, J.N., Kemp, K.C., Perman, J.A., Bourlinos, A.B., Kim, K.S., Zboril, R.: Noncovalent functionalization of graphene and graphene oxide for energy materials, biosensing, catalytic, and biomedical applications. Chem. Rev. **116**, 5464–5519 (2016)

Gupta, B.D., Sharma, A.K.: Sensitivity evaluation of a multi-layered surface plasmon resonance-based fiber optic sensor: a theoretical study. Sens. Actuators B Chem. **107**, 40–46 (2005)

Hao, H., Li, H., Wang, S., Cheng, Z., Fang, Y.: Epitaxial growth of Ag-Cu bimetallic nanoparticles via thermal evaporation deposition. Appl. Surf. Sci. **505**, 143871 (2020)

He, Y., Xing, X., Tang, H., Pang, D.: Graphene oxide-based fluorescent biosensor for protein detection via terminal protection of small-molecule-linked DNA. Small **9**, 2097–2101 (2013)

Homola, J., Piliarik, M.: Surface plasmon resonance (SPR) sensors. In: Surface Plasmon Resonance Based Sensors, pp. 45–67. Springer, Berlin (2006)

Kumar, A., Yadav, A.K., Kushwaha, A.S., Srivastava, S.: A comparative study among WS2, MoS2 and graphene based surface plasmon resonance (SPR) sensor. Sens. Actuators Rep. **2**, 100015 (2020)

Kumar, A., Kumar, A., Kushwaha, A.S., Dubey, S.K., Srivastava, S.: A comparative study of different types of sandwiched structures of SPR biosensor for sensitive detection of ssDNA. Photonics Nanostruct. Fundam. Appl. **48**, 100984 (2022a)

Kumar, A., Kumar, A., Srivastava, S.: Silicon nitride-BP-based surface plasmon resonance highly sensitive biosensor for virus SARS-CoV-2 detection. Plasmonics **17**(3), 1065–1077 (2022b)

Kumar, A., Kumar, A., Srivastava, S.: A Study on surface plasmon resonance biosensor for the detection of CEA biomarker using 2D materials graphene, Mxene and MoS$_2$. Optik **258**, 168885 (2022c)

Kushwaha, A.S., Kumar, A., Kumar, R., Srivastava, M., Srivastava, S.: Zinc oxide, gold and graphene-based surface plasmon resonance (SPR) biosensor for detection of pseudomonas like bacteria: a comparative study. Optik **172**, 697–707 (2018a)

Kushwaha, A.S., Kumar, A., Kumar, R., Srivastava, S.: A study of surface plasmon resonance (SPR) based biosensor with improved sensitivity. Photonics Nanostr. Fundam. Appl. **31**, 99–106 (2018b)

Li, M.-H., Wang, Y.-S., Cao, J.-X., Chen, S.-H., Tang, X., Wang, X.-F., Zhu, Y.-F., Huang, Y.-Q.: Ultrasensitive detection of uranyl by graphene oxide-based background reduction and RCDzyme-based enzyme strand recycling signal amplification. Biosens. Bioelectron. **72**, 294–299 (2015)

Liu, Z., Tabakman, S., Welsher, K., Dai, H.: Carbon nanotubes in biology and medicine: in vitro and in vivo detection, imaging and drug delivery. Nano Res. **2**, 85–120 (2009)

Liu, J., Qin, Y., Li, D., Wang, T., Liu, Y., Wang, J., Wang, E.: Highly sensitive and selective detection of cancer cell with a label-free electrochemical cytosensor. Biosens. Bioelectron. **41**, 436–441 (2013)

Liu, C., Cai, Q., Xu, B., Zhu, W., Zhang, L., Zhao, J., Chen, X.: Graphene oxide functionalized long period grating for ultrasensitive label-free immunosensing. Biosens. Bioelectron. **94**, 200–206 (2017)

Loh, K.P., Bao, Q., Eda, G., Chhowalla, M.: Graphene oxide as a chemically tunable platform for optical applications. Nat. Chem. **2**, 1015–1024 (2010)

Luke, K., Okawachi, Y., Lamont, M.R., Gaeta, A.L., Lipson, M.: Broadband mid-infrared frequency comb generation in a Si_3N_4 microresonator. Opt. Lett. **40**, 4823–4826 (2015)

Manawi, Y.M., Samara, A., Al-Ansari, T., Atieh, M.A.: A review of carbon nanomaterials' synthesis via the chemical vapor deposition (CVD) method. Materials **11**, 822 (2018)

Masson, J.-F.: Surface plasmon resonance clinical biosensors for medical diagnostics. ACS Sens. **2**, 16–30 (2017)

Maurya, J., Prajapati, Y., Singh, V., Saini, J., Tripathi, R.: Performance of graphene–MoS2 based surface plasmon resonance sensor using silicon layer. Opt. Quant. Electron. **47**, 3599–3611 (2015)

Morales-Luna, G., Morales-Luna, M.: Effective medium theory to the description of plasmonic resonances: role of Au and Ti nanoparticles embedded in MoO_3 thin films. Sci. Rep. **10**, 1–12 (2020)

Mruk, D.D., Cheng, C.Y.: Enhanced chemiluminescence (ECL) for routine immunoblotting: an inexpensive alternative to commercially available kits. Spermatogenesis **1**, 121–122 (2011)

Mudgal, N., Saharia, A., Choure, K.K., Agarwal, A., Singh, G.: Sensitivity enhancement with anti-reflection coating of silicon nitride (Si3N4) layer in silver-based surface plasmon resonance (SPR) sensor for sensing of DNA hybridization. Appl. Phys. A **126**, 1–8 (2020a)

Mudgal, N., Saharia, A., Agarwal, A., Singh, G.: ZnO and Bi-metallic (Ag–Au) layers based surface plasmon resonance (SPR) biosensor with $BaTiO_3$ and graphene for biosensing applications. IETE J. Res. (2020b). https://doi.org/10.1080/03772063.2020.1844074

Notarangelo, L.D., Fischer, A., Geha, R.S., Casanova, J.-L., Chapel, H., Conley, M.E., Cunningham-Rundles, C., Etzioni, A., Hammartröm, L., Nonoyama, S.: Primary immunodeficiencies: 2009 update. J. Allergy Clin. Immunol. **124**, 1161–1178 (2009)

Peelaers, H., Chabinyc, M., Van de Walle, C.: Controlling n-type doping in MoO_3. Chem. Mater. **29**, 2563–2567 (2017)

Rahman, M.M., Rana, M.M., Rahman, M.S., Anower, M., Mollah, M.A., Paul, A.K.: Sensitivity enhancement of SPR biosensors employing heterostructure of PtSe2 and 2D materials. Opt. Mater. **107**, 110123 (2020)

Raikwar, S., Prajapati, Y.K., Srivastava, D.K., Saini, J.P.: Graphene oxide based SPR sensor for sensing of sea water concentration. Results Opt. **1**, 100011 (2020)

Schasfoort, R.B.: Handbook of Surface Plasmon Resonance. Royal Society of Chemistry, Cambridge (2017)

Singh, M.K., Pal, S., Prajapati, Y.K., Saini, J.P.: Sensitivity improvement of surface plasmon resonance sensor on using BlueP/MoS 2 heterostructure and antimonene. IEEE Sens. Lett. **4**, 1–4 (2020)

Singh, V., Late, D.J., Goyal, A., Rath, S.: Raman spectroscopic investigations of the selenization of MoO3 in the chemical vapor deposition process to form two-dimensional MoSe2. Appl. Surf. Sci. **538**, 147946 (2021)

Soga, T., Ohashi, Y., Ueno, Y., Naraoka, H., Tomita, M., Nishioka, T.: Quantitative metabolome analysis using capillary electrophoresis mass spectrometry. J. Proteome Res. **2**, 488–494 (2003)

Song, J., Xu, L., Zhou, C., Xing, R., Dai, Q., Liu, D., Song, H.: Synthesis of graphene oxide based CuO nanoparticles composite electrode for highly enhanced nonenzymatic glucose detection. ACS Appl. Mater. Interfaces **5**, 12928–12934 (2013)

Srivastava, A., Prajapati, Y.K.: Effect of sulfosalt and polymers on performance parameter of SPR biosensor. Opt. Quant. Electron. **52**, 1–14 (2020)

Stelling, C., Singh, C.R., Karg, M., König, T.A., Thelakkat, M., Retsch, M.: Plasmonic nanomeshes: their ambivalent role as transparent electrodes in organic solar cells. Sci. Rep. **7**, 1–13 (2017)

Tang, Y., Zeng, X., Liang, J.: Surface plasmon resonance: an introduction to a surface spectroscopy technique. J. Chem. Educ. **87**, 742–746 (2010)

Thomas, T., Jayababu, N., Shruthi, J., Mathew, A., Cerdán-Pasarán, A., Hernández-Magallanes, J.A., Sanal, K., Reshmi, R.: Room temperature ammonia sensing of α-MoO_3 nanorods grown on glass substrates. Thin Solid Films **722**, 138575 (2021)

Uthanna, S., Nirupama, V., Pierson, J.: Substrate temperature influenced structural, electrical and optical properties of dc magnetron sputtered MoO3 films. Appl. Surf. Sci. **256**, 3133–3137 (2010)

Wang, Y., Li, Z., Wang, J., Li, J., Lin, Y.: Graphene and graphene oxide: biofunctionalization and applications in biotechnology. Trends Biotechnol. **29**, 205–212 (2011)

Wu, Q., Song, D., Zhang, D., Sun, Y.: An enhanced SPR immunosensing platform for human IgG based on the use of silver nanocubes and carboxy-functionalized graphene oxide. Microchim. Acta **183**, 2177–2184 (2016)

Xiong, X., Chen, Y., Wang, H., Hu, S., Luo, Y., Dong, J., Zhu, W., Qiu, W., Guan, H., Lu, H.: Plasmonic interface modified with graphene oxide sheets overlayer for sensitivity enhancement. ACS Appl. Mater. Interfaces **10**, 34916–34923 (2018)

Xue, T., Cui, X., Chen, J., Liu, C., Wang, Q., Wang, H., Zheng, W.: A switch of the oxidation state of graphene oxide on a surface plasmon resonance chip. ACS Appl. Mater. Interfaces **5**, 2096–2103 (2013)

Yang, Z.-W., Pham, T.-T.-H., Hsu, C.-C., Lien, C.-H., Phan, Q.-H.: Single-layer-graphene-coated and gold-film-based surface plasmon resonance prism coupler sensor for immunoglobulin G detection. Sensors **22**, 1362 (2022)

Zhang, S., Wang, K., Li, K.-B., Shi, W., Jia, W.-P., Chen, X., Sun, T., Han, D.-M.: A DNA-stabilized silver nanoclusters/graphene oxide-based platform for the sensitive detection of DNA through hybridization chain reaction. Biosens. Bioelectron. **91**, 374–379 (2017)

Zheng, Y., Lang, T., Cao, B., Jin, J., Dong, R., Feng, H.: Fiber optic SPR sensor for human Immunoglobulin G measurement based on the MMF-NCF-MMF structure. Opt. Fiber Technol. **46**, 179–185 (2018)